Proceedings of the Combustion Institute 40 (2024) 105489

Contents lists available at ScienceDirect

Proceedings of the Combustion Institute

journal homepage: www.elsevier.com/locate/proci

High pressure ammonia/methanol oxidation up to 100 atm

Ziyu Wang [a], Bowen Mei [a,*], Ning Liu [a], Andy Thawko [a], Xingqian Mao [a], Hao Zhao [a], Peter Glarborg [b], Stephen J. Klippenstein [c], Yiguang Ju [a]

[a] Department of Mechanical and Aerospace Engineering, Princeton University, Princeton, NJ 08544, USA
[b] Department of Chemical and Biochemical Engineering, Technical University of Denmark (DTU), Lyngby DK-2800, Denmark
[c] Chemical Sciences and Engineering Division, Argonne National Laboratory, Lemont, IL 60439, USA

ARTICLE INFO

Keywords:
Ammonia
Methanol
N_2O/NO_x/HONO
Supercritical pressure jet-stirred reactor
Ultra-high pressure

ABSTRACT

High pressure ammonia/methanol oxidation and NO_x formations were investigated using a recently developed supercritical pressure jet-stirred reactor (SP-JSR) at 20 and 100 atm with temperatures between 550 and 950 K and equivalence ratios of 0.138 and 1.15. The experimental results show that NH_3 oxidation at high pressure is significantly accelerated by the active OH radicals produced from CH_3OH oxidation. Furthermore, the kinetic interactions between NH_3 and CH_3OH are governed mainly by the reactions $CH_3OH + NH_2 = CH_2OH + NH_3$, $CH_3OH + NH_2 = CH_3O + NH_3$, and $CH_2O + NH_2 = HCO + NH_3$. A HP-Mech model for high-pressure NH_3/CH_3OH oxidation was developed in this study. It consists of the most recent NH_3 and CH_3OH models including some new reactions and updated rate constants from the literature as well as NH_3-CH_3OH interactions where rate constants of $CH_3OH + NH_2 = CH_2OH + NH_3$, $CH_3OH + NH_2 = CH_3O + NH_3$, $NH_2 + CH_2O = NH_3 + HCO$, and $NH_2 + CH_2O = NH_2CHO + H$ were theoretically calculated in this study. Our model with these updates improves the prediction for the measured N_2O/NO_x temperature dependence at 100 atm. In addition, the reaction pathway and sensitivity analysis show that N_2O/NO_x/HONO interactions with HO_2 are very important, especially for a fuel-lean mixture at 100 atm. The HONO mole fraction for the fuel-lean mixture at 100 atm was then measured by off-axis integrated cavity output spectroscopy (ICOS) at wavenumber of 6638.26 cm^{-1}. The experimental data show a significant HONO formation at intermediate temperature that is strongly underpredicted by numerical simulation at 100 atm. Therefore, the HONO related reactions with notable uncertainty at high pressure such as $NO + OH (+M) = HONO (+M)$ and $H_2NO + NO_2 = HONO + HNO$ need deeper exploration in the future.

1. Introduction

With the clear societal need to curb greenhouse gas emissions and mitigate anthropogenic climate change, it is imperative to develop carbon-neutral fuels. Ammonia (NH_3) is a carbon-neutral fuel and an attractive hydrogen (H_2) carrier that is increasingly recognized as a sustainable energy source for transportation, power generation, and storage in recent years [1,2], provided that ammonia is synthesized from renewable energy [3]. However, utilization of ammonia as a fuel remains a challenge due to its low reactivity and possibly high NO_x emission at high pressure. Therefore, blending NH_3 with methanol (CH_3OH) provides an attractive prospective resolution to this issue. Furthermore, CH_3OH is easily dissolved in NH_3 and is an attractive E-fuel [4–6]. A sustainable closed-carbon cycle shows that CH_3OH can be synthesized from renewable H_2 and atmospheric CO_2 [7].

Ammonia oxidation has been explored extensively in recent decades. It has been summarized in the literature comprehensively [8] and will not be reviewed herein. However, NH_3/CH_3OH oxidation has not been well-studied, with only a few works including laminar flame speed [9], ignition delay time [10–12], species measurements in a jet-stirred reactor [13], and kinetic modeling study [14–16] available in the literature. The details of the oxidation and NO_x formations have not been characterized experimentally under the high/ultra-high pressure Otto cycle engine conditions (above 10 atm/up to 100 atm). Combustion at such pressures is an emerging technique for lowering pollutant emissions and enhancing thermodynamic efficiency [17]. Furthermore, intermolecular forces, multi-body collisions, and real gas effects under such conditions may cause significant uncertainties in the rate constants calculated using the classical transition state theory as well as thermodynamic and transport properties based on the ideal gas law. Therefore, it is valuable to conduct kinetics experiments of NH_3/CH_3OH oxidation and NO_x formations at pressures up to 100 atm and to develop a detailed

* Corresponding author.
E-mail address: bowenm@princeton.edu (B. Mei).

https://doi.org/10.1016/j.proci.2024.105489
Received 3 December 2023; Accepted 19 June 2024
Available online 24 July 2024

chemical kinetic model.

Recently, Zhao et al. [18] developed a supercritical pressure jet-stirred reactor (SP-JSR) at Princeton University for conducting kinetic studies under extreme pressure (up to 200 atm). It provides a valuable platform complementary to the high-pressure shock tube [19,20] and the high-pressure laminar flow reactor [21,22] for performing kinetic experiments. The SP-JSR operates over a wide range of high pressures (10–200 atm) and low to intermediate temperatures (295–1200 K), and with a homogenous turbulent mixing, uniform temperature distribution, and well-defined flow residence time [23].

As such, in this work, NH_3/CH_3OH oxidation and NO_x formations were investigated at pressures of 20 and 100 atm, at temperatures between 550 and 950 K, and at fuel-air equivalence ratios of 0.138 and 1.15 by using our SP-JSR. The mole fractions of CH_3OH, NH_3, N_2O, NO, HONO, and other key species were quantified by micro-gas/gas chromatography (μ-GC/GC) and laser absorption spectroscopy. Numerical simulations were performed with the Perfectly Stirred Reactor (PSR) module in CHEMKIN software. The experimental data were compared with four kinetic models and the coupling effects of NH_3/CH_3OH oxidation on fuel consumption and NO_x formations were investigated for up to 100 atm in fuel-rich and fuel-lean mixtures. Furthermore, a HP-Mech model for high pressure NH_3/CH_3OH oxidation was developed with the most recent amine subset including some new reactions and updated rate constants from the literature as well as theoretically calculated in this study. Besides, the high-pressure chemistry of NH_3/CH_3OH was analyzed by using the HP-Mech model in this study.

2. Experimental setup and kinetic models

Fig. 1 displays the schematic setup of the SP-JSR system coupled with multiple diagnostic devices. The core part is a spherical quartz reactor located inside a stainless-steel shell. The reactor has internal volume of 0.4 cm^3 with four jet fingers. Each jet finger has two perpendicular nozzles with 200 μm inner diameter, which can create intense turbulence and homogenous mixing [23]. The gas flows (N_2, O_2, NH_3, Airgas, ≥99.998 % purity) were supplied by the high-pressure mass flow controllers (Brooks, SLA5800) and the liquid fuel (CH_3OH, Sigma-Aldrich, ≥99.9 % purity) was injected into a vaporization line by a high-pressure syringe pump (Harvard PHD). The pressures inside and outside the reactor were controlled by a back pressure regulator and were balanced by the bath N_2 flow. The electric heating wires with PID controllers were installed inside and outside of the stainless-steel shell to maintain the uniform temperature distribution (+/-5 K) in the reactor. More details of this setup are described in our previous paper [18].

As shown in Fig. 1, CH_3OH, CO, CO_2, H_2O, and CH_2O were quantified by a μ-GC Thermal Conductivity Detector (TCD, INFICON 3000) within 5 % uncertainty, NH_3 and N_2O were quantified by GC Nitrogen Chemiluminescence Detector (NCD, Agilent 8890) within 5 % uncertainty, NO was measured by tunable diode laser absorption spectroscopy (TDLAS) in a multi-pass Herriot cell at wavenumber of 1726.4 cm^{-1} within 5 %

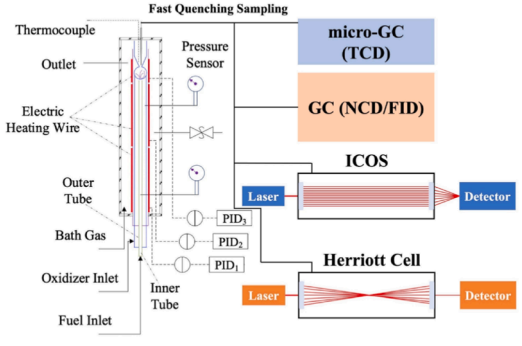

Fig. 1. Schematic setup of SP-JSR system.

uncertainty [24], HONO was measured by off-axis integrated cavity output spectroscopy (ICOS) at wavenumber of 6638.26 cm^{-1} with an uncertainty of 42 % [25]. The experimental uncertainty is mainly due to the estimated errors of the absorption cross-section of HONO at this wavenumber [26].

As listed in Table 1, we performed the experiments with fixed NH_3 to CH_3OH ratio (3.75 to 1) at 20 and 100 atm for both fuel-rich and fuel-lean mixtures. To minimize the errors in flow control and perturbation, the mixture volume flow rates (295 K and 1 atm) were fixed at 0.8 L/min (case 1) and 4 L/min (cases 2 and 3). Therefore, the flow residence time ($\tau\,[s] = 177/T\,[K]$) varies with each temperature and the range of flow residence time stays the same at different pressures.

The experimental data obtained in the SP-JSR were compared with the following kinetic models: Li et al. [10], He et al. [13], Zhang et al. [15], and HP-Mech (this study). The HP-Mech consists of our most recent updated high pressure CH_3OH [27] and NH_3 [28] models. Several new reactions such as $NH_2 + O = NO + H_2$, $HNO + H (+M) = HNOH (+M)$, $H_2NO (+M) = H_2 + NO (+M)$, $HNOH (+M) = H_2NO (+M)$ calculated by Klippenstein et al. [29] were added and rate constants of existing reactions related to NH_2, HNO, H_2NO were updated from the literature [29–31]. The interaction reactions of NH_3 and CH_3OH were also adopted from the literature [10]. The rate constants of $CH_3OH + NH_2 = CH_2OH + NH_3$, $CH_3OH + NH_2 = CH_3O + NH_3$, $NH_2 + CH_2O = NH_3 + HCO$, and $NH_2 + CH_2O = NH_2CHO + H$ were theoretically calculated in this study. The detailed calculation method is described in the following section and more information on the HP-Mech model can be referred to Table S1 in the Supplementary Material. The numerical simulations were performed with the Perfectly Stirred Reactor module in Ansys Chemkin-Pro software at a constant temperature. Calculations indicate that the real gas effect in this work is very small even at 100 atm (cf. Fig. S1 in the Supplementary Material).

3. Theoretical prediction of rate constants

The rovibrational properties of the stationary points on the potential energy surfaces for NH_2 reacting with CH_3OH and with CH_2O (cf. Figs. S2 and S3 in the Supplementary Material) were mapped out at the CCSD(T)-F12/cc-pVTZ-F12 level. The energies were then mapped out with a composite method that approximates the ANL0 method. In particular, the present composite energies consist of (i) CCSD(T)-F12 complete basis set (CBS) estimates (two point extrapolation from cc-pVQZ-F12 and cc-pV5Z-F12 bases), (ii) CCSDT(Q)/cc-pVDZ corrections, (iii) CCSD(T)/CBS core-valence corrections (two point extrapolation from cc-pCVTZ and cc-pCVQZ bases), (iv) CCSD(T)/aug-cc-pwCVTZ Douglas-Kroll relativistic corrections, and (v) B2PLYP-D3/cc-pVTZ anharmonic corrections (from second order vibrational perturbation theory). The B2PLYP-D3/cc-pVTZ method was used to explore the intrinsic reaction coordinate MEPs and projected frequencies for each of the kinetically relevant transition states.

The present 'ANL0-TZF' calculations differ only slightly from our earlier ANL0-F12 approach [32], with similar expected 2σ accuracies of about 0.2 kcal/mol. The primary difference involves the use of the higher accuracy explicitly correlated CCSD(T)-F12/cc-pVTZ-F12 method in place of the CCSD(T)/cc-pVTZ method in the determination of the geometries and harmonic frequencies. The CCSD(T)-F12 basis set extrapolation is also based on explicit calculations for one higher level in the basis sets (i.e., QZ-F12 and 5Z-F12 in place of TZ-F12 and QZ-F12). Extrapolation coefficients of 0.9 and 0.6 were used in the CBS(QZF,5ZF) and CBS(TZ,QZ) extrapolations, respectively. Other reasonable extrapolations would yield differences of no more than a few hundredths of a kcal/mol.

Coupled cluster calculations were performed with the MOLPRO software [33], except for the DBOC corrections, which were obtained with CFOUR [34]. The MRCC module from Kallay [35] was used within MOLPRO to obtain the CCSDT(Q) corrections. Meanwhile, the B2PLYP-D3 density functional theory calculations were performed with

Table 1
Experimental conditions.

Case	Pressure (atm)	Temperature (K)	Equivalence ratio	NH_3 (%)	CH_3OH (%)	O_2 (%)	N_2 (%)	Residence time (s)
1	20	550–950	1.15	0.375	0.1	0.375	99.15	0.32–0.19
2	100	550–900	1.15	0.375	0.1	0.375	99.15	0.32–0.2
3	100	550–900	0.138	0.375	0.1	3.125	96.4	0.32–0.2

Gaussian 16 [36]. Detailed descriptions can be found in the Supplementary Material.

Rate predictions were obtained from 1-dimensional master equations incorporating the aforementioned ab initio transition state properties within transition state theory (TST) based determinations of the fluxes for the individual reaction channels. The TST calculations included Eckart tunneling corrections, one-dimensional hindered rotor treatments for the relevant torsional motions, B2PLYP-D3 evaluations of variational corrections, and vibrational anharmonic corrections obtained through incorporation of anharmonic corrections to the fundamental frequencies in place of the harmonic frequencies. For both systems, the rates were found to be effectively pressure independent. The present ab initio transition state theory-based predictions for the rate constants for NH_2 to react with CH_3OH and with CH_2O are well reproduced over the 500–2500 K range by the following modified Arrhenius fits: $7.44T^{3.64}\exp(-4300/RT)$, $NH_2 + CH_3OH = NH_3 + CH_2OH$; $1.86T^{3.59}\exp(-2930/RT)$, $NH_2 + CH_3OH = NH_3 + CH_3O$; $1.38 \times 10^4 T^{2.15}\exp(-1750/RT)$, $NH_2 + CH_2O = NH_2CHO + H$; $806T^{3.08}\exp(-1550/RT)$, $NH_2 + CH_2O = NH_3 + HCO$, where the rate constants are in $cm^3\ mole^{-1}\ s^{-1}$, T is in K, and R is in cal $mole^{-1}\ K^{-1}$.

Variational and anharmonic effects are minimal (15 % or less) for both channels in the reaction of NH_2 with CH_3OH. Tunneling is more significant, increasing the rate constants by a factor of two or more up until about 700 K. The tunneling corrections only decay to 20 % at about 1200 K.

The total rate constant predicted by Giri et al. [37] for the $NH_2 + CH_3OH$ reaction is remarkably similar to that reported here, while that reported by Li et al. [10] is about an order of magnitude lower (cf. Fig. S4). These prior studies employed electronic structure methods that were similar to each other and obtained similar barrier heights, but that are considerably less definitive and distinct from the present ones. Furthermore, the kinetic methodologies were similar. Thus, it is somewhat surprising that the rate constants differ by as much as they show.

The present predictions for the branching ratio in the $NH_2 + CH_3OH$ reaction indicate a nearly equal branching ratio between CH_3O and CH_2OH near room temperature that gradually begins to favor the production of CH_2OH with increasing temperature. The studies of Li et al. [10] and Giri et al. [37] also suggested that the CH_2OH products were increasingly favored with room temperature, but Li et al. [10] predict a much lower branching, while Giri et al. [37] predict a much higher branching (cf. Fig. S5). It is perhaps worth stating that the much higher levels of electronic structure theory employed in the present work should make the present predictions for the rate constants and branching ratios considerably more reliable than those of these earlier studies. We would estimate 2σ uncertainties for the present work of about a factor of 1.5 for temperatures of most relevance to combustion.

Anharmonic effects on the vibrational partition function are again minimal (20 % or less) for both channels in the reaction of NH_2 with CH_2O. Variational effects for the abstraction to produce $NH_3 + HCO$ are predicted to be about 2 % or less, while those for the addition/elimination to produce $NH_2CHO + H$ are more substantive, and gradually increase in importance with increasing temperature. Near 1000 K, the latter variational correction reduces the rate constant by about 25 %. This correction increases to a 60 % reduction by 2000 K.

Both Li et al. [38] and Douglas et al. [39] predict significantly smaller total rate constants for the $NH_2 + CH_2O$ reaction (cf. Fig. S6), as might be expected given their predicted higher barriers. The present work and Douglas et al. are in agreement that the $NH_3 + HCO$ channel is only a minor channel (cf. Fig. S7). The present calculations suggest that the maximum branching ratio to this channel is only about 5 %. Again, the present work employs much higher levels of electronic structure theory and so should be considered more reliable. We would estimate 2σ uncertainties for the present work of about a factor of 1.5 for temperatures of most relevance to combustion.

4. Results and discussion

Fig. 2(a) and (b) depict the mole fractions of NH_3 and CH_3OH versus temperature at 20 atm for Case 1 in Table 1. The black squares indicate the experimental data, and the curves with different colors indicate the numerical simulations using different kinetic models. It is seen that the onset temperature of CH_3OH consumption at 20 atm is around 775 K and the onset temperature of NH_3 consumption at 20 atm is around 800 K, which is much faster than pure NH_3 oxidation due to the higher reactivity of CH_3OH. The oxidation of CH_3OH at lower temperatures provides active OH radicals to accelerate the NH_3 oxidation via $NH_3 + OH = NH_2 + H_2O$. As to the numerical simulations at 20 atm, the Li et al. [10], He et al. [13], and Zhang et al. [15] models slightly overpredict the NH_3 consumption, while HP-Mech (this study) model slightly underpredict the NH_3 consumption. It is because we added several new reactions such as $NH_2 + O = NO + H_2$, $HNO + H (+M) = HNOH (+M)$, $H_2NO (+M) = H_2 + NO (+M)$, $HNOH (+M) = H_2NO (+M)$ [29] and updated rate constants of several existing reactions related to NH_2, HNO, H_2NO from the literature [29–31]. However, all models underpredicted the CH_3OH consumption, which is consistent with our previous work [27]. In our previous study, we updated the rate constants of a few key reactions in HO_2 chemistry including $CH_3OH + HO_2 = CH_2OH + H_2O_2$, $CH_2O + HO_2 = HOCH_2O_2$, $H_2O_2 (+M) = 2OH (+M)$, $HO_2 + HO_2 = 2OH + O_2$, which results in the improvement of CH_3OH profile prediction below 800 K [27].

Fig. 3 depicts the mole fractions of NH_3 and CH_3OH versus temperature at 100 atm for Case 2 (a) and Case 3 (b) of Table 1, respectively. Experimental results show that the onset temperature of NH_3 consumption at 100 atm is in the range of 750–775 K and the onset temperature of CH_3OH consumption at 100 atm is around 725 K, which is 50 K lower than that at 20 atm. Furthermore, it can be noted that the oxidation of NH_3 and CH_3OH is faster for the fuel-lean condition than the fuel-rich condition at 100 atm. This is because the fuel-lean mixture

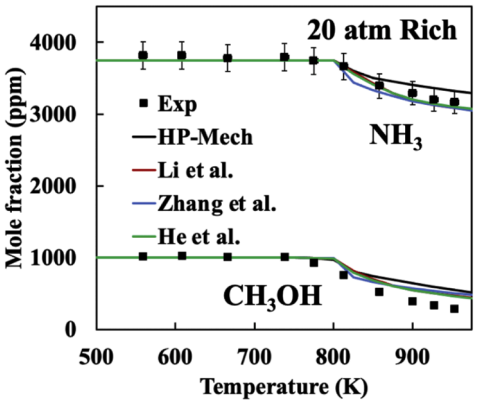

Fig. 2. Temperature evolutions of (a) NH3 and (b) CH3OH mole fractions for fuel-rich mixture (Case 1).

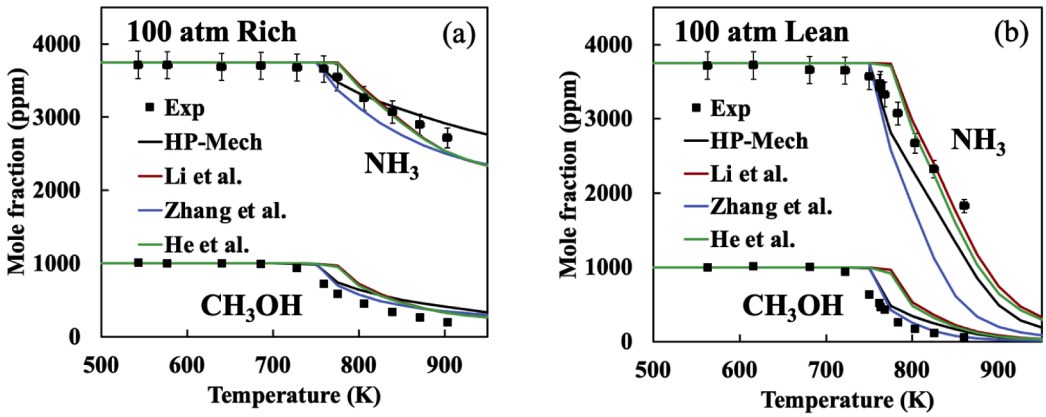

Fig. 3. Temperature evolutions of NH3 and CH3OH mole fractions for (a) fuel-rich (Case 2) and (b) fuel-lean (Case 3) mixtures.

has higher O_2 concentration, which enhances the reactions related to HO_2 chemistry, including $CH_3OH + HO_2 = CH_2OH + H_2O_2$, $CH_2O + HO_2 = HOCH_2O_2$, $H_2O_2 (+M) = 2OH (+M)$, $HO_2 + HO_2 = 2OH + O_2$, especially at high pressure. As to the numerical simulations at 100 atm, the Li et al. [10] and He et al. [13] models underpredict NH_3 oxidation, while the model from Zhang et al. overpredicts NH_3 oxidation. The HP-Mech model has the best prediction among these four models; however, it slightly overpredicts NH_3 oxidation for fuel-lean mixture over 800 K. Similar to the case at 20 atm, all models underpredict CH_3OH oxidation for the fuel-rich mixture above 800 K at 100 atm. Nevertheless, the difference in the onset temperature of CH_3OH consumption between experimental data and numerical simulation is around 50 K, which is consistent with our previous work [27].

Fig. 4(a)–(f) depict the mole fractions of other key species at 100 atm for the fuel-lean mixture, i.e., N_2O, NO, CO, CO_2, CH_2O, and H_2O. It can be noted that the HP-Mech model has the best overall prediction compared to other models, consistent with the predictions of NH_3 and CH_3OH. Nevertheless, the model overpredicts N_2O and H_2O formations at temperatures above 800 K and slightly underpredicts CH_2O formation. This result means that the model overpredicts the overall reactivity of NH_3 oxidation above 800 K and underpredicts the overall reactivity of CH_3OH oxidation. A discrepancy is also noted for the experimental and numerical simulation results for CO and CO_2 production. The model overpredicts CO formation and underpredicts CO_2 formation, which is also consistent with our previous results for methanol at 100 atm [27]. It implies that some important reactions involved in CO and CO_2, such as $CO + HO_2 = CO_2 + OH$, $CO + OH = HOCO$, $CO + OH = CO_2 + H$, $HCO (+M) = H + CO (+M)$, and $CO + N_2O = N_2 + CO_2$ need more careful evaluation for ultra-high-pressure conditions. In addition, the numerical simulations show that almost 100 % of carbon from CH_3OH converts to CO, CO_2, and CH_2O at temperatures above 800 K. However, only around 80 % of the carbon from CH_3OH converts to CO, CO_2, and CH_2O according to the experimental data. This result implies that some C—N species may exist under ultra-high-pressure conditions due to the interaction of NH_3-CH_3OH and advanced diagnostics is required for further investigation.

To further investigate the coupling effects of high pressure NH_3/CH_3OH oxidation, a reaction pathway analysis was performed for NH_3 and CH_3OH consumptions. The HP-Mech model was selected for this analysis based on its superior model performance. Fig. 5 illustrates the reaction pathways of NH_3/CH_3OH fuel-lean mixture at 100 atm and 800 K for case 3 in Table 1. It is seen that the H-abstractions from NH_3 and CH_3OH by OH are the dominant first-step reactions. The H-abstraction from CH_3OH by NH_2 is also very important due to the kinetic interaction between CH_3OH and NH_3. Nevertheless, the H-abstraction from CH_3OH by HO_2 is much less important compared to pure CH_3OH oxidation [27]. This change in importance between these two reactions is because CH_3OH has a higher reaction rate with NH_2 than HO_2 even when HO_2

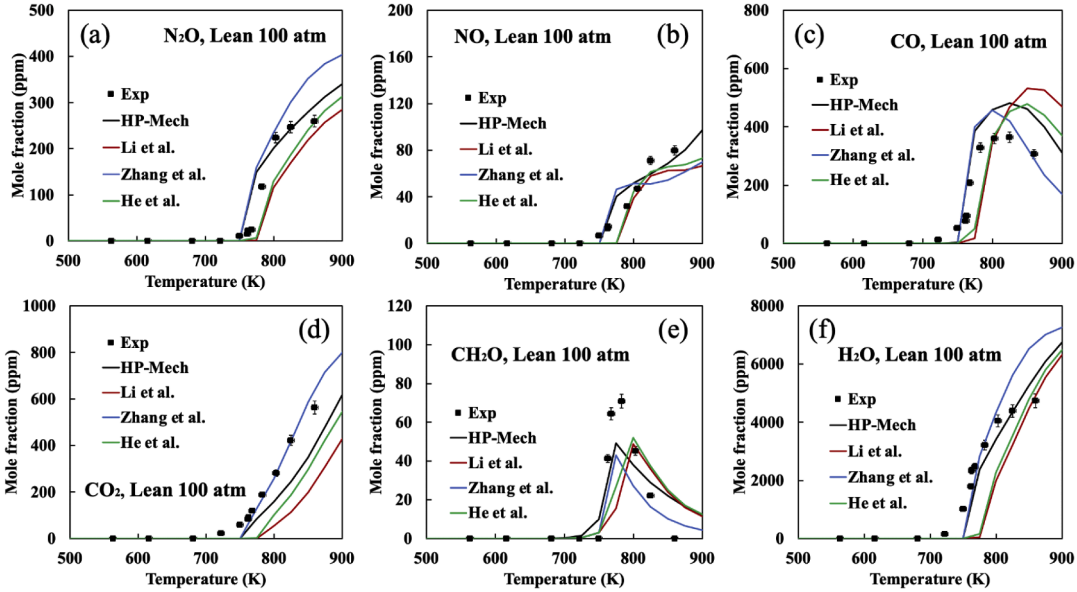

Fig. 4. Temperature evolutions of (a) N2O, (b) NO, (c) CO, (d) CO2, (e) CH2O, and (f) H2O mole fractions for fuel-lean mixture (Case 3).

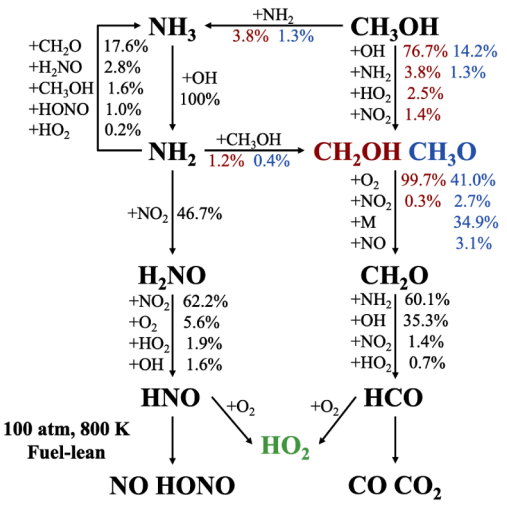

Fig. 5. Reaction pathways for NH3/CH3OH fuel-lean oxidation at 100 atm and 800 K using the HP-Mech model.

production is increased at high pressure. It can be also noted that the production of CH_2OH (84.4 %, red font in Fig. 5) is much higher than CH_3O (15.5 %, blue font in Fig. 5) because the C–H bond on the methyl site is weaker than the alternative O–H bond [40]. The key intermediate species H_2NO in NH_3 oxidation and the key intermediate species CH_2O in CH_3OH oxidation are mainly formed by $NH_2 + NO_2 = H_2NO + NO$, and $CH_2OH + O_2 = CH_2O + HO_2$, respectively. Then, the production of HNO is governed by $H_2NO + NO_2 = HNO + HONO$, and the production of small species HCO is governed by $CH_2O + NH_2 = HCO + NH_3$ and $CH_2O + OH = HCO + H_2O$. Unlike pure CH_3OH oxidation [27], $CH_2O + NH_2 = HCO + NH_3$ (60.1 %) is more important than $CH_2O + OH = HCO + H_2O$ (35.3 %) and $CH_2O + HO_2 = HCO + H_2O_2$ (0.7 %) due to the interaction of NH_3 and CH_3OH. At last, the major pathways of HO_2 formation are $HNO + O_2 = HO_2 + NO$, $HCO + O_2 = HO_2 + CO$, and $CH_2OH + O_2 = CH_2O + HO_2$. The details of $NO_x/N_2O/HONO/HO_2$ interactions and reaction pathways will be discussed in a later section.

To explore the discrepancy between experiment and numerical simulation, a sensitivity analysis was performed for NH_3 and CH_3OH. Fig. 6(a) and (b) display the sensitivity coefficients of major reactions at 100 atm and 800 K for fuel-lean (red) and fuel-rich (blue) mixtures, respectively. It can be noted from Fig. 6(a) that the reactions $NH_2 + NO_2 = H_2NO + NO$, $HNO + O_2 = HO_2 + NO$, and $NH_2 + NO = NNH + OH$ are the three most sensitive for promoting NH_3 oxidation, while the chain-termination reactions $NH_2 + NO_2 = N_2O + H_2O$, $HNO + NO_2 = HONO + NO$, and $NH_2 + NO = N_2 + H_2O$ are the most sensitive steps for inhibiting NH_3 oxidation. It can be also noted from Fig. 6(b) that the reactions of $NH_2 + NO_2$ and $NH_2 + NO$ show the same behavior in the sensitivity analysis of CH_3OH as in that of NH_3. Furthermore, the chain-propagating reaction $CH_3OH + OH = CH_2OH + H_2O$ is the most sensitive one for promoting CH_3OH oxidation, which confirms the statement in the reaction pathway analysis. The reactions related to HONO turn out to be very important, especially for fuel-lean mixtures. Possibly the discrepancy between the experiment and numerical simulation for NH_3 at fuel-lean condition is, to some extent, due to the uncertainties of the reactions related to HONO in the current kinetic model. Therefore, it is valuable to measure the formation of HONO.

Fig. 7(a) displays the temperature evolution of HONO for the fuel-lean mixture at 100 atm measured by off-axis integrated cavity output spectroscopy (ICOS) at wavenumber of 6638.26 cm^{-1}. Both experimental data and numerical simulation show that there is significant HONO formation and the HONO formation first increases with temperature and then decreases after a peak between 775 and 800 K. We understand the experimental uncertainty of this measurement is up to 42 % mainly due to the estimated errors of the absorption cross-section of HONO at this wavenumber [25,26]. However, it is seen that all four models significantly underpredict the experimental data, which is in the 100–200 ppm level (2.6–5.3 % of the nitrogen content in NH_3). To explore this discrepancy a reaction pathway analysis was performed for HONO formation and consumption with the HP-Mech model. Fig. 7(b) illustrates the HONO reaction pathways at 100 atm and 800 K. HONO is

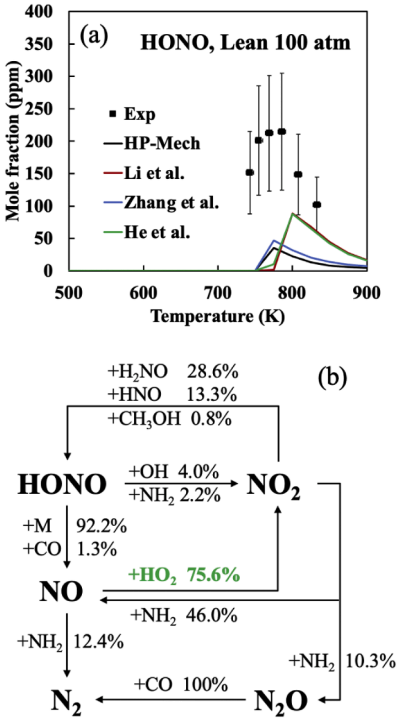

Fig. 7. (a) Temperature evolution of HONO mole fraction measured by ICOS (b) HONO reaction pathways at 100 atm and 800 K using HP-Mech model.

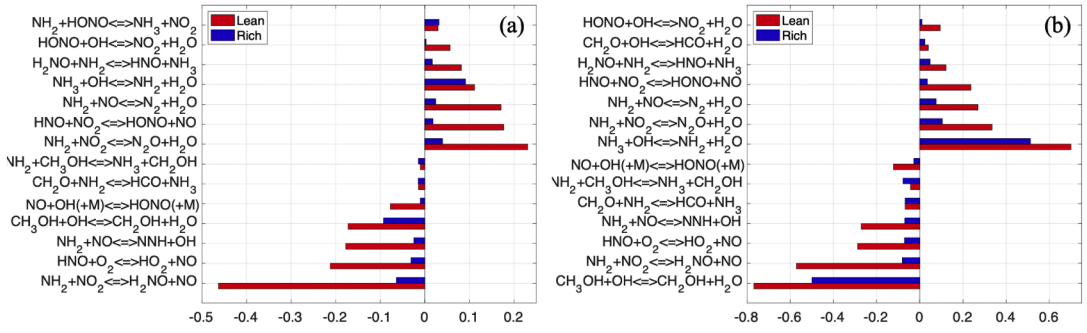

Fig. 6. Sensitivity analysis for (a) NH_3 (b) CH_3OH in NH_3/CH_3OH oxidation at 100 atm and 800 K using HP-Mech model.

mainly produced from NO_2 through reactions $NO_2 + H_2NO = HONO + HNO$ and $NO_2 + HNO = HONO + NO$. HONO is mainly converted to NO through $HONO (+M) = NO + OH(+M)$. NO_2 is produced from NO through $NO + HO_2 = NO_2 + OH$, with HO_2 mainly produced by $HNO + O_2 = HO_2 + NO$. Therefore, the NO_x kinetics coupled with HO_2 at high pressure is very important to HONO reaction pathway. The major HONO formation reactions have a negative effect on NH_3 consumption as shown in Fig. 6. This result means that the underprediction of HONO formation by numerical simulation is consistent with the overprediction of NH_3 consumption for fuel-lean mixture at 100 atm. Therefore, the HONO related reactions with notable uncertainty at high pressure $NO + OH (+M) = HONO (+M)$ and $H_2NO + NO_2 = HONO + HNO$ need deeper exploration.

5. Conclusions

The supercritical pressure jet-stirred reactor (SP-JSR) provides a new platform for conducting kinetic studies at extreme pressures. NH_3/CH_3OH oxidation and NO_x formations were studied in our SP-JSR at pressures of 20 and 100 atm, temperatures ranging from 550 to 950 K, and equivalence ratios of 0.138 and 1.15.

The results show that NH_3 oxidation is strongly accelerated by the active OH radicals produced from CH_3OH oxidation through $NH_3 + OH = NH_2 + H_2O$. Furthermore, the major coupling reactions between NH_3 and CH_3OH are $CH_3OH + NH_2 = CH_2OH + NH_3$, $CH_3OH + NH_2 = CH_3O + NH_3$, and $CH_2O + NH_2 = HCO + NH_3$. In this study, we developed a new HP-Mech model for high-pressure NH_3/CH_3OH oxidation including the most recent NH_3 model, CH_3OH model, and NH_3-CH_3OH interaction subset where rate constants of $CH_3OH + NH_2 = CH_2OH + NH_3$, $CH_3OH + NH_2 = CH_3O + NH_3$, $NH_2 + CH_2O = NH_3 + HCO$, and $NH_2 + CH_2O = NH_2CHO + H$ were theoretically calculated in this study. Several new reactions such as $NH_2 + O = NO + H_2$, $HNO + H (+M) = HNOH (+M)$, $H_2NO (+M) = H_2 + NO (+M)$, $HNOH (+M) = H_2NO (+M)$ were added and rate constants of existing reactions related to NH_2, HNO, H_2NO were updated from the literature. Our model improves the prediction for the experimental data at 100 atm and reproduces well the RCM and shock tube derived ignition delay times from the literature. In addition, the results show that N_2O-NO_x-HONO interactions with HO_2 are very important through $HNO + O_2 = HO_2 + NO$, $NO + HO_2 = NO_2 + OH$, and $NO_2 + H_2NO = HONO + HNO$ for the fuel-lean mixture at 100 atm. We measured the concentration of HONO by off-axis integrated cavity output spectroscopy (ICOS) at wavenumber of 6638.26 cm^{-1}. The experimental data of HONO formation was significantly underpredicted by numerical simulation at 100 atm. Based on the model analysis, the HONO related reactions with notable uncertainty at high pressure such as $NO + OH (+M) = HONO (+M)$ and $H_2NO + NO_2 = HONO + HNO$ need deeper exploration in the future.

Declaration of competing interest

The authors declare that they have no known competing financial interests or personal relationships that could have appeared to influence the work reported in this paper.

Acknowledgments

This work was partly funded by the DOE BES award DE-SC0021135. B. Mei would like to appreciate the partial financial support from Shanghai Jiao Tong University for his postdoctoral fellowship. A. Thawko gratefully acknowledges the financial support of the Israeli Council for Higher Education - Planning and Budgeting Committee. The material in this study is based in part on work at ANL supported by the U. S. Department of Energy (USDOE), Office of Basic Energy Sciences, Division of Chemical Sciences, Geosciences, and Biosciences under DOE Contract Number DE-AC02–06CH11357 through the Argonne-Sandia Consortium on Pressure Dependent Chemistry, FWP 59044.

Supplementary materials

Supplementary material associated with this article can be found, in the online version, at doi:10.1016/j.proci.2024.105489.

The supplementary material submitted along with the manuscript includes the HP-Mech model developed in this study, detailed descriptions of theoretical rate prediction methods and results, experimental data, and supplementary figures comparing model and experiment.

References

[1] A. Valera-Medina, H. Xiao, M. Owen-Jones, W.I. David, P. Bowen, Ammonia for power, Prog. Energy Combust. Sci. 69 (2018) 63–102.
[2] H. Kobayashi, A. Hayakawa, K.D.K.A. Somarathne, E.C. Okafor, Science and technology of ammonia combustion, Proc. Combust. Inst. 37 (2019) 109–133.
[3] Q. Dong, Y. Yao, S. Cheng, K. Alexopoulos, J. Gao, S. Srinivas, Y. Wang, Y. Pei, C. Zheng, A.H. Brozena, H. Zhao, X. Wang, H.E. Toraman, B. Yang, I.G. Kevrekidis, Y. Ju, D.G. Vlachos, D. Liu, L. Hu, Programmable heating and quenching for efficient thermochemical synthesis, Nature 605 (2022) 470–476.
[4] A.K. Agarwal, Biofuels (alcohols and biodiesel) applications as fuels for internal combustion engines, Prog. Energy Combust. Sci 33 (2007) 233–271.
[5] S. Jenkins, Methanol production from natural gas, Chem. Eng. (N.Y.) 123 (2016) 37.
[6] K. Kumabe, S. Fujimoto, T. Yanagida, et al., Environmental and economic analysis of methanol production process via biomass gasification, Fuel 87 (2008) 1422–1427.
[7] G.A. Olah, A. Goeppert, G.K.S. Prakash, Chemical recycling of carbon dioxide to methanol and dimethyl ether: from greenhouse gas to renewable, environmentally carbon neutral fuels and synthetic hydrocarbons, J. Org. Chem. 74 (2009) 487–498.
[8] P. Glarborg, J.A. Miller, B. Ruscic, S.J. Klippenstein, Modeling nitrogen chemistry in combustion, Prog. Energy Combust. Sci. 67 (2018) 31–68.
[9] Z. Wang, X. Han, Y. He, R. Zhu, Y. Zhu, Z. Zhou, K. Cen, Experimental and kinetic study on the laminar burning velocities of NH_3 mixing with CH_3OH and C_2H_5OH in premixed flames, Combust. Flame 229 (2021) 111392.
[10] M. Li, X. He, H. Hashemi, P. Glarborg, V.M. Lowe, P. Marshall, R. Fernandes, B. Shu, An experimental and modeling study on auto-ignition kinetics of ammonia/methanol mixtures at intermediate temperature and high pressure, Combust. Flame 242 (2022) 112160.
[11] X. Li, Z. Ma, Y. Jin, X. Wang, Z. Xi, S. Hu, X. Chu, Effect of methanol blending on the high-temperature auto-ignition of ammonia: an experimental and modeling study, Fuel 339 (2023) 126911.
[12] S. Nadiri, B. Shu, C.F. Goldsmith, R. Fernandes, Development of comprehensive kinetic models of ammonia/methanol ignition using Reaction Mechanism Generator (RMG), Combust. Flame 251 (2023) 112710.
[13] X. He, M. Li, B. Shu, R. Fernandes, K. Moshammer, Exploring the effect of different reactivity promoters on the oxidation of ammonia in a jet-stirred reactor, J. Phys. Chem. A 127 (2023) 1923–1940.
[14] H. Xu, J. Wang, C. Zhang, L. Dai, Z. He, Q. Wang, Combustion chemistry of ammonia/C1 fuels: numerical study on laminar burning velocity of ammonia flame with methanol addition, Int. J. Hydrog. Energy 47 (2022) 28152–28164.
[15] X. Zhang, K.K. Yalamanchi, S.M. Sarathy, Combustion chemistry of ammonia/C1 fuels: a comprehensive kinetic modeling study, Fuel 341 (2023) 127676.
[16] M. Lu, D. Dong, F. Wei, W. Long, Y. Wang, L. Cong, P. Dong, H. Tian, P. Wang, Chemical mechanism of ammonia-methanol combustion and chemical reaction kinetics analysis for different methanol blends, Fuel 341 (2023) 127697.
[17] G.P. Sutton, O. Biblarz, Rocket Propulsion Elements, John Wiley & Sons, 2016.
[18] H. Zhao, C. Yan, T. Zhang, G. Ma, M.J. Souza, C. Zhou, Y. Ju, Studies of high-pressure n-butane oxidation with CO_2 dilution up to 100 atm using a supercritical-pressure jet-stirred reactor, Proc. Combust. Inst. 38 (2021) 279–287.
[19] G. Kogekar, C. Karakaya, G.J. Liskovich, et al., Impact of non-ideal behavior on ignition delay and chemical kinetics in high-pressure shock tube reactors, Combust. Flame 189 (2018) 1–11.
[20] J. Shao, R. Choudhary, D.F. Davidson, et al., Ignition delay times of methane and hydrogen highly diluted in carbon dioxide at high pressures up to 300 atm, Proc. Combust. Inst. 37 (2019) 4555–4562.
[21] R.X. Fernandes, K. Luther, J. Troe, Falloff curves for the reaction $CH_3 + O_2 (+ M) \rightarrow CH_3O_2 (+ M)$ in the pressure range 2-1000 bar and the temperature range 300-700 K, J. Phys. Chem. A 110 (2006) 4442–4449.
[22] C.L. Rasmussen, J. Hansen, P. Marshall, P. Glarborg, Experimental measurements and kinetic modeling of $CO/H_2/O_2/NO_x$ conversion at high pressure, Int. J. Chem. Kinet. 40 (2008) 454–480.
[23] H. Zhao, M. Souza, Y. Ju, Fusion, J. Am. Sci. Glass-Blowers Soc. 66 (2018) 19–24.
[24] H. Zhong, X. Mao, N. Liu, Z. Wang, T. Ombrello, Y. Ju, Understanding non-equilibrium N_2O/NO_x chemistry in plasma-assisted low-temperature NH_3 oxidation, Combust. Flame 256 (2023) 112948.
[25] L. Marrodán, Y. Song, O. Herbinet, M.U. Alzueta, C. Fittschen, Y. Ju, F. Battin-Leclerc, First detection of a key intermediate in the oxidation of fuel + NO systems: HONO, Chem Phys Lett 719 (2019) 22–26.
[26] C. Jain, P. Morajkar, C. Schoemaecker, B. Viskolcz, C. Fittschen, Measurement of absolute absorption cross sections for nitrous acid (HONO) in the near-infrared

region by the continuous wave cavity ring-down spectroscopy (cw-CRDS) technique coupled to laser photolysis, J. Phys. Chem. A 115 (2011) 10720–10728.
[27] Z. Wang, H. Zhao, C. Yan, Y. Lin, A.D. Lele, W. Xu, B. Rotavera, A.W. Jasper, S. J. Klippenstein, Y. Ju, Methanol oxidation up to 100 atm in a supercritical pressure jet-stirred reactor, Proc. Combust. Inst. 39 (2023) 445–453.
[28] L.S. Thorsen, M.S.T. Jensen, M.S. Pullich, J.M. Christensen, H. Hashemi, P. Glarborg, V.A. Alekseev, E.J.K. Nilsson, Z. Wang, B. Mei, N. Liu, Y. Ju, High pressure oxidation of NH_3/n-heptane mixtures, Combust. Flame 254 (2023) 112785.
[29] S.J. Klippenstein, C.R. Mulvihill, P. Glarborg, Theoretical kinetics predictions for reactions on the NH_2O potential energy surface, J. Phys. Chem. A 127 (2023) 8650–8662.
[30] A. Stagni, C. Cavallotti, H-abstractions by O_2, NO_2, NH_2, and HO_2 from H_2NO: theoretical study and implications for ammonia low-temperature kinetics, Proc. Combust. Inst. 39 (2023) 633–641.
[31] J. Jian, H. Hashemi, H. Wu, P. Glarborg, A.W. Jasper, S.J. Klippenstein, An experimental, theoretical, and kinetic modeling study of post-flame oxidation of ammonia, Combust. Flame 261 (2023) 113325.
[32] S.J. Klippenstein, L.B. Harding, B. Ruscic, Ab initio computations and active thermochemical tables hand in hand: heats of formation of core combustion species, J. Phys. Chem. A 121 (2017) 6580–6602.
[33] H.J. Werner, P.J. Knowles, G. Knizia, F.R. Manby, M. Schutz, Molpro: a general-purpose quantum chemistry program package, WIREs Comput. Mol. Sci. 2 (2012) 242–253.
[34] D.A. Matthews, L. Cheng, M.E. Harding, F. Lipparini, S. Stopkowicz, T.C. Jagau, P. G. Szalay, J. Gauss, J.F. Stanton, Coupled-cluster techniques for compuational chemistry: the CFOUR program package, J. Chem. Phys. 152 (2020) 214108.
[35] M. Kállay, P.R. Surján, Higher excitations in coupled-cluster theory, J. Chem. Phys. 115 (2001) 2945–2954.
[36] M.J. Frisch, G.W. Trucks, H.B. Schlegel, G.E. Scuseria, M.A. Robb, J.R. Cheeseman, G. Scalmani, V. Barone, B. Mennucci, G.A. Petersson, et al., Gaussian 09, Revision D.01, Gaussian, Inc., Wallingford CT, 2009.
[37] B.R. Giri, K.P. Shrestha, T.V.T. Mai, F. Mauss, L.K. Huynh, A theoretical kinetic study of the reactions of NH2 radicals with methanol and ethanol and their implications in kinetic modeling, Int. J. Chem. Kinet. 55 (2023) 3–14.
[38] Q.S. Li, R.H. Lu, Direction dynamics study of the hydrogen abstraction reaction $CH_2O + NH_2 = CHO + NH_3$, J. Phys. Chem. A 106 (2002) 9446–9450.
[39] K.M. Douglas, D.I. Lucas, C. Walsh, N.A. West, M.A. Blitz, D.E. Heard, The gas-phase reaction of NH_2 with Formaldehyde (CH_2O) is not a source of formamide (NH_2CHO) in interstellar environments, Astrophys. J. Lett. 937 (2022) L16.
[40] U. Burke, W.K. Metcalfe, S.M. Burke, K.A. Heufer, P. Dagaut, H.J. Curran, A detailed chemical kinetic modeling, ignition delay time and jet-stirred reactor study of methanol oxidation, Combust. Flame 165 (2016) 125–136.